Structural Engineering and Mechanics, Vol. 18, No. 6 (2004) 791-806
DOI: http://dx.doi.org/10.12989/sem.2004.18.6.791

Experiment study of structural random loading identification by the inverse pseudo excitation method

Xing-Lin Guo† and Dong-Sheng Li‡

Department of Engineering Mechanics, Dalian University of Technology, Dalian 116024, China

(Received May 11, 2004, Accepted July 13, 2004)

Abstract. The inverse pseudo excitation method is used in the identification of random loadings. For structures subjected to stationary random excitations, the power spectral density matrices of such loadings are identified experimentally. The identification is based on the measured acceleration responses and the structural frequency response functions. Numerical simulation is used in the optimal selection of sensor locations. The proposed method has been successfully applied to the loading identification experiments of three structural models, two uniform steel cantilever beams and a four-story plastic glass frame, subjected to uncorrelated or partially correlated random excitations. The identified loadings agree quite well with actual excitations. It is proved that the proposed method is quite accurate and efficient in addition to its ability to alleviate the ill conditioning of the structural frequency response functions.

Key words: loading identification; inverse pseudo excitation method; random vibration; computer simulation.

1. Introduction

Three typical problems exist for a linear structure subjected to multiple stationary random excitations. The first is the analysis of structural responses due to given excitations, for stationary random excitations, the power spectral density (PSD) matrices of the responses are usually computed. This so-called "direct problem" can be solved efficiently by the pseudo excitation method (PEM) (Lin *et al.* 1992, 1994). The second is the system identification problem, for which the properties of a structure are identified from the known PSD functions of both loadings and response. As viewed from experimental modal analysis, this is to extract structural dynamic properties (resonant frequencies, mode shapes and modal damping ratios) from the frequency response functions (FRFs). The FRFs are obtained by measuring the excitations and the corresponding responses (Ewins 1984). Many publications cover such system identification problems and their successful applications in engineering (Juang 1994). The third is the so-called loading identification problem, for which the PSD functions of the responses and the properties of the structure (FRF) are known as a prior and will be used in the identification of the loadings. This "inverse problem" has received much less attention in the literature. Some similar work has been done at a high expense, but quite few results were published because of the poor precision. In fact, loading identification is

† Professor
‡ Ph.D. Candidate

very important, and many loads in engineering applications need be identified. For instance, the traffic loads of bridges; the seismic excitations of buildings; the interaction forces between moving machines and their bases, and so on. Such excitations are very difficult or even impossible to measure directly. However, the excited responses are sometimes more easily to measure, and therefore, will be used in the identification of the excitations.

Investigations for loading identification are carried out with emphasis in various fields. The earliest was conducted by Barlett *et al.* (Barlett and Flannelly 1979) to determine the external vibratory forces exerted on the rotor hub of a helicopter dynamic model. Subsequently, Giansante *et al.* (1982) tested on a real AH-1G helicopter to reconstruct the magnitudes and phase angles of in-flight rotor vibratory forces acting on the airframe from acceleration responses and mobility calibration matrix. Hillary and Ewins (1984) tested a simple cantilever beam by using two sinusoidal forces of the same frequency but different magnitudes. Their experiment results showed that the poor identification of forces were caused largely by the contamination of measurement noise, and that strain gauge measurement, instead of accelerometer, will improve the reconstructed excitations in the lower frequency range to some extent. Moreover, Okubo *et al.* (1985) tested three different kinds of real structures: a machine tool, an automobile engine and an air conditioner under operating conditions, and reached a good agreement between the identified and actual forces. They also analyzed different influences of noises on the identified results using a synthesized model. In above tests, the method of direct inversion of FRF, by which the loadings are computed by the multiplication of the responses and the inverted FRF matrices, is used.

In addition to the direct inversion of FRF, modal coordinate transformation method was developed for loading identification. The modal coordinates, derived by several orders of mode shapes, were first implemented to decouple the governing equations of motion of a structure with multiple degree of freedoms, then the pseudo-inverse technique was employed to compute the force vector in the modal space. Finally, the actual loadings were computed by transforming this force vector back into the original coordinates. Using this method, Desanghere and Snoeys (1985) conducted identification experiments on a real longitudinal beam of a car frame excited by three electro-magnetic shakers. They also studied the influences of noise contamination, perturbation of modal parameters and limited number of modes on the identification results by an analytical model. However, the modal coordinate transformation method is drastically weakened by the insufficiency of the participating modes, in particular by the lack of the higher order modes that are hard to obtain accurately for an actual structure.

In above experiments, the locations of the input forces are all known, which is prerequisite for loading identification. Callahan *et al.* (1994) discussed a situation in which the input locations are not known and found that the forces are adequately determined when the assumed forces locate where actual forces act; otherwise, the identified forces are distributed evenly to all the locations in the assumed set. Moreover, Avitabile and Chandler (2001) studied on how to optimally place sensors in loading identification. They proposed a Test Reference Identification Procedure for the selection of multiple reference locations by a pre-modal test with a very limited set of potential reference locations. This procedure was developed mainly because a finite element model (FEM) may be inaccurate, and if it is used to identify reference locations for tests, then it may not produce the best results or even miss modes.

Besides loading identification in the frequency domain, force identification can also be approached in the time domain based on the system impulse response function. Adams and Doyle (2002) developed a recursive formulation to identify impact force time history combined with a finite

element model, and conducted identification experiments on a cylindrical shell and a one-sided Hopkinson Bar. Zhu and Law (2002) adopted a regularization method to overcome the ill-conditioning and to stabilize the unbonded solution for the identification of moving loadings on a continuous beam from strains and accelerations. Two thorough reviews concerning different methods and existing problems of loading identification literature can be found in Karl (1987) and Dobson *et al.* (1990).

However, most of the above explorations dealt only with the identification of deterministic forces, for instance impact forces. For random excitations, the identified results using these methods are not satisfactory. The inverse pseudo excitation method (IPEM) is proved effective in identifying such random loadings in principle (Lin *et al.* 2001), and will be further justified via experiments in this paper. Using this method, the response PSD matrix at a given frequency is first decomposed to produce a pseudo response vector, which will then be used to generate a pseudo excitation vector by means of a corresponding FRF. Finally, the loading PSD matrices are reconstructed by multiplication of such pseudo excitation vectors in an appropriate form.

In this paper, the IPEM method and the associated theory is described. The computer simulation scheme for the optimal selection of sensor locations, as well as the experiment results for loading identification are also presented. The IPEM yielded excellent identification results in the experiments with two cantilever beams with different damping ratios, and a frame made of plastic glass. The experimental results are used to the analysis of the identification precision. Part of the work was first appeared in IMAC XXI (Li *et al.* 2003).

2. Theory of the inverse pseudo excitation method

For a linear structure subjected to stationary random vibrations, the fundamental formula, which relates the response PSD matrices with the excitation PSD matrices by FRFs in the frequency domain, is given by (Newland 1984).

$$[S_{yy}] = [H]^{*}[S_{xx}][H]^{T} \tag{1}$$

In which $[S_{xx}]$ is the known excitation PSD matrix, $[H]$ is the FRF matrix, and $[S_{yy}]$ is the response PSD matrix. The superscripts * and T represent complex conjugate and transpose, respectively.

Eq. (1) is used for computing the responses of a structure subjected to known excitations in the direct problem. Conversely for an inverse problem of loading identification, the responses of a structure are already given and are used to compute the unknown excitations. The known response PSD matrix $[S_{yy}]$ can generally be assumed to be a $p \times p$ Hermitian matrix with rank r ($\leq p$), and can be decomposed into the following form,

$$[S_{yy}] = \sum_{j=1}^{r} \{b\}_j^{*} \{b\}_j^{T} \tag{2}$$

Eq. (2) can generally be realized in terms of the spectral decomposition scheme or Cholesky decomposition of the Hermitian matrix. If $[S_{yy}]$ consists of only real quantities, then $\{b\}_j$ is simplified into the product of the square root of the jth eigen-value and corresponding mass normalized eigen-vector of the response PSD matrix obtained by a common matrix eigen-value computation.

Assuming the structure is excited by a pseudo excitation, $\{x\}_j = \{a\}_j e^{i\omega t}$, the pseudo response vector can be expressed by the pseudo excitation vector as:

$$\{b\}_j e^{i\omega t} = [H]\{x\}_j = [H]\{a\}_j e^{i\omega t} \tag{3}$$

$$\{a\}_j = [H]^+ \{b\}_j \tag{4}$$

where the superscript + represents a Moore-Penrose generalized inversion. Clearly,

$$\sum_{j=1}^{r} \{a\}_j^* \{a\}_j^T = \sum_{j=1}^{r} \{[H]^+ \{b\}_j\}^* \{[H]^+ \{b\}_j\}^T = [H]^{+*} \sum_{j=1}^{r} \{b\}_j^* \{b\}_j^T [H]^{+T} = [H]^{+*} [S_{yy}] [H]^{+T} \tag{5}$$

Hence, by substituting Eq. (1) into Eq. (5), the excitation PSD matrix $[S_{xx}]$ can be expressed in terms of $\{a\}_j$ as

$$[S_{xx}] = \sum_{j=1}^{r} \{a\}_j^* \{a\}_j^T \tag{6}$$

Eq. (6), i.e., the IPEM, is obviously accurate in theory, and it is quite efficient because each FRF matrix at a specific frequency need be inverted only once.

In general, the determination of n external excitations requires m ($m \geq n$) measured responses, and the inversion of the $m \times n$ FRF matrix may often meet ill-conditioning problem. The singular value decomposition (SVD) scheme (Golub and Van Loan 1996) is employed in the inversion process of the FRF matrix as follows,

$$[H] = [U][S][V]^H \tag{7}$$

where, the superscript H represents a transposed conjugate, $[U]$ represents the left singular matrix corresponding to the matrix of mode shapes, $[S]$ is the diagonal singular value matrix, and $[V]$ represents the right singular matrix corresponding to the matrix of mode participations.
Thus,

$$[H]^+ = [V][S]^+ [U]^H \tag{8}$$

Consequently, the test steps for experimental loading identification are set up following equations from Eqs. (2)-(8) in combination with computer simulation for optimal sensor placement.

(1) Computer simulation for sensor placement. Select several candidate sets of different response measurement points, assume an excitation matrix, and simulate the identification result as well as the condition numbers of FRF matrices. Choose the best set of sensor locations that has the smallest discrepancies between the assumed and reconstructed loadings and that has the lowest overall condition numbers of FRFs.

(2) System or FRF matrix calibration. Generate the FRF matrices by artificially exciting the structure at the significant frequency points of external loadings. For each excitation, the force and the accelerations at selected measurement locations are measured and stored through a data acquisition card in a laptop computer simultaneously, and are later processed to yield one column of the FRF matrix in sequence. With all the loading points excited, a complete FRF matrix is obtained.

(3) Responses measuring. Measure all the responses simultaneously under normal vibratory conditions. Establish the response PSD matrices from measured acceleration time history using Fast Fourier Transform (FFT) algorithm (Bendat and Piersol 2000). Meanwhile, the actual excitations, which are used later for the comparison of the identified excitations with the original ones as references, are also measured by force transducers in the experiments.

(4) Loading reconstruction. Inverse the FRF matrices using the SVD scheme (Eqs. (7) and (8)) at the discrete frequencies, decompose the measured response PSD matrices to obtain a pseudo response vector (Eq. (2)), multiply the inversion of the FRF matrix and the pseudo response vector to get a pseudo excitation vector (Eq. (4)). Reconstruct the excitation PSD matrices by Eq. (5).

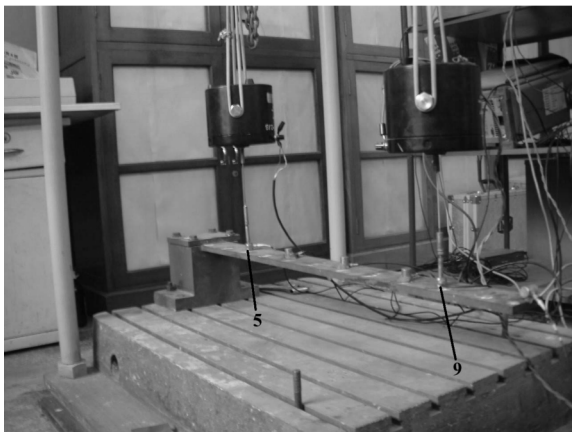

Fig. 1 Steel cantilever beam

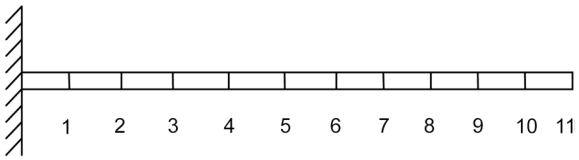

Fig. 2 Finite element model of the steel cantilever beam

Fig. 3 Plastic glass cantilever beam

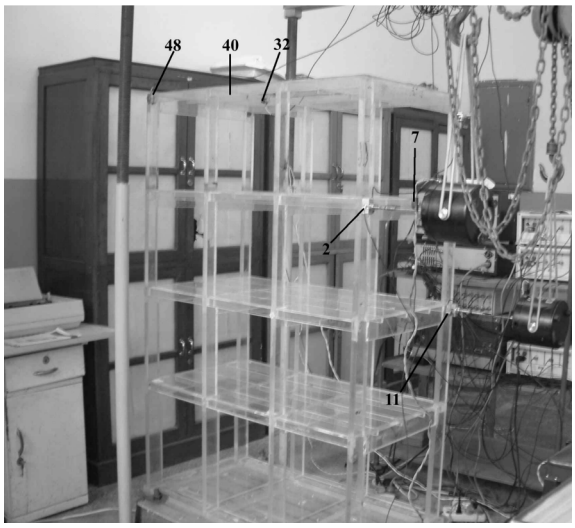

Fig. 4 Plastic glass frame

Three structures were tested in this paper. The first was a uniform steel cantilever beam and its length, width and thickness are 88.5 cm, 7.5 cm and 1.2 cm respectively (Fig. 1). Fig. 2 shows it's analytical model and FEM mesh discretization. The second was an erect uniform plastic glass cantilever beam with the same size as the steel cantilever beam (Fig. 3). The third was a four-story frame made of plastic glass, which was the model of a building (Fig. 4). The frame, having dimensions of 0.9 × 0.48 × 1.37 m (L × W × H), has four floors, and each floor has four bays. This frame is comparatively complicated and was chosen to test the feasibility of applying IPEM on complex engineering structures.

3. Selection of measurement locations

Selection of measurement locations before conducting experiments by means of computer simulation is an efficient approach in improving identification effect. Usually, the initial candidate sensor locations are based on heurism in Lin *et al.* (2001). In this paper, however, such initial candidate sensor locations are selected more rigorously in accordance with the modal kinetic energy (MKE), by which all the possible candidate locations are ranked in descending order according to their MKE values. The MKE values of each candidate location are computed using the following relation

$$\mathrm{MKE}_{in} = \Phi_{in} \sum_{j} M_{ij} \Phi_{jn} \tag{9}$$

Where, MKE is the kinetic energy associated with the ith degree of freedom in the nth target mode, Φ_{in} is the ith component in the corresponding mode, M_{ij} is the term in the ith row and jth column of the FEM mass matrix, and Φ_{jn} is the jth element of the nth mode. The first six target mode shapes, which are adequate to identify structural loadings as shown in the following experiment section, are involved in the computation of MKE values. For the first model, all the eleven candidate locations are ranked in descending order according to their MKE values as follows: 11,6,5,9,7,2,8,3,10,1.

Then in the second step, computer simulation for loading identification is performed to optimally select sensor locations. By computer simulation, first choose four locations with largest MKE values and assume to apply excitations at the places where the structure are excited (Point 5, 9). The assumed excitation PSD matrix at all given discrete frequencies is:

$$[S_{xx}] = \begin{bmatrix} 2.0 & 0 \\ 0 & 1.0 \end{bmatrix} \tag{10}$$

Compute the corresponding FRF matrices by an FEM program for the four locations preliminarily selected by MKE method. The response power spectrum density (PSD) matrices are then computed by implementing PEM. These response PSD matrices are further used to generate the excitation PSD matrices based on the IPEM. Repeat this process for the preliminary selected combinations of sensor locations in sequence, compare the identified excitation PSD matrices with the assumed loading spectrum as well as the condition numbers of the FRF matrices for each set, the best one with smallest disparities between identified and assumed excitations and overall condition numbers will be used in later experiments.

The results of computer simulation for the first candidate set (locations at 11,9,8,5) are shown in Fig. 5(a) and another set of sensor locations at 11,9,6,5 are in Fig. 5(b). Clearly, the first set are

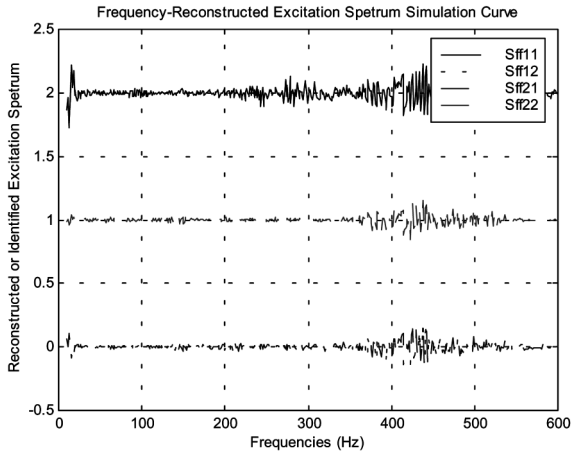

Fig. 5 (a) Measured points at 5,8,9,11

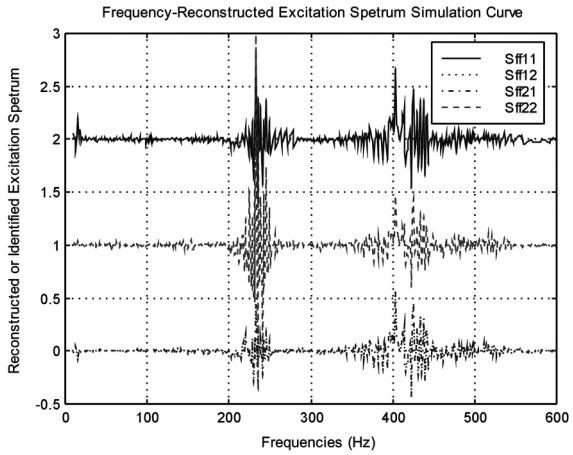

Fig. 5 (b) Measured points at 5,6,9,11

better than that of the second set since the range of abnormal jumps in Fig. 5(b) is much broader and the amplitude is comparatively higher than that in Fig. 5(a). Obviously, the simulation results are quite different even though only one measurement location is different. The locations 7 and 2 are excluded in the simulation because the coherence coefficients between the excitation and the response at these two points are lower than that at location 8 in actual modal tests. As a result, the optimal sensor locations for loading identification of the steel cantilever beam are 11,9,8,5.

It should be noted that computer simulation may still be usable even if the analytical model of a structure can not be established properly. The reason for this situation is the inability of mathematical modeling techniques to adequately describe the structure because of inaccurate material parameters or impractical boundary conditions. In such cases, FRF matrices are measured experimentally, and other related procedures remain the same in the simulation process. For the models of Fig. 3 and Fig. 4, such FRF matrices should be measured experimentally because the properties of plastic glass are usually unstable, and the joints in the frame are not connected rigidly.

4. Experiment results of random loading identification

4.1 Experiment system setup

A 16-channel data acquisition system (DAQ), INV306D intelligent signal acquisition and analysis system, was employed for the measurement of accelerations as well as excitations. The DAQ system is fully digital, multi-channel and computerized. Electrical signals from the two force transducers (B&K842424, B&K842425) and four acceleration sensors (YD-70Bs) are converted into digital forms and stored in the hard disk of a laptop computer, which performs the conventional FFT procedure, FRF and auto- or cross- power density spectrum computation with the DASP 6.0 software supplied with INV306D. The simulation and later identification computation are based on Matlab5.0. Moreover, an HP35670A was used for instant experiment setup check for the validation of reciprocity, initial FRFs and coherence functions analysis to assure the quality of the data acquired.

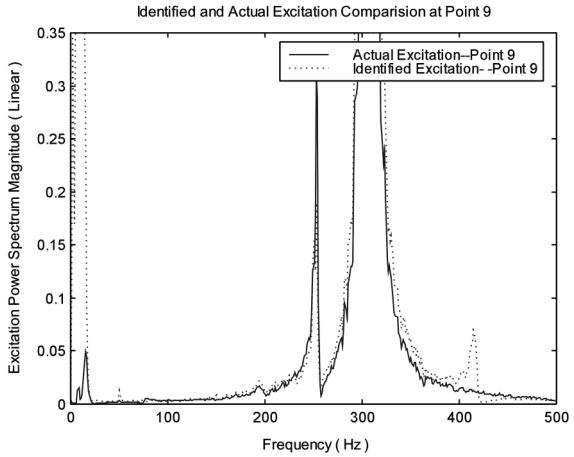

Fig. 6 (a) Point 9 reconstructed and actual force

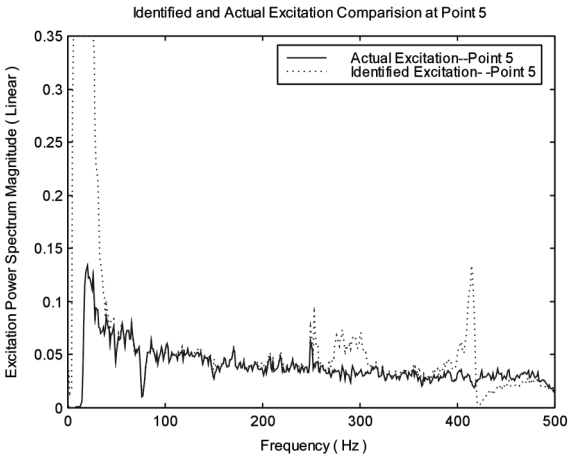

Fig. 6 (b) Point 5 reconstructed and actual force

4.2 Steel cantilever beam

Two uncorrelated excitations were applied at points 5,9 vertically and four acceleration responses were measured at 5,8,9,11 simultaneously (Fig. 1). The significant frequency range is from 0 to 500 Hz, which includes the first four natural frequencies. As a whole, the identified excitations (Fig. 6a and Fig. 6b) agree with the actual ones quite well.

The reconstructed excitations below 10Hz were poor partly because the sensitivity of the accelerometers used is low in this frequency range and partly because the resonant frequencies of the suspension system of the two shakers and the support structures of the beam also fell in this range. As recommended in Ewins (1984), strain gages were possibly used to make some improvements. Fig. 6(c) and Fig. 6(d) show the FRFs and coherence functions between the two

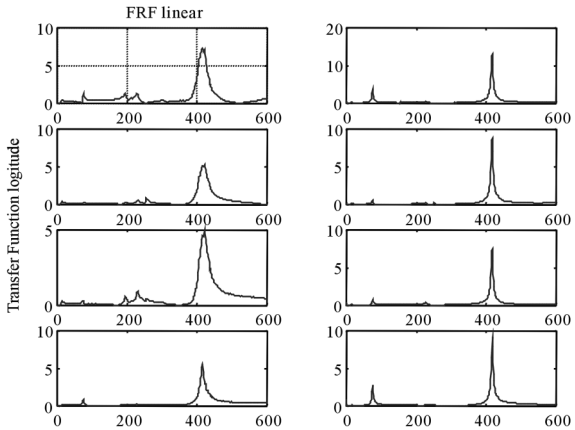

Fig. 6 (c) Frequency response function (First column corresponds to the 1st excitation)

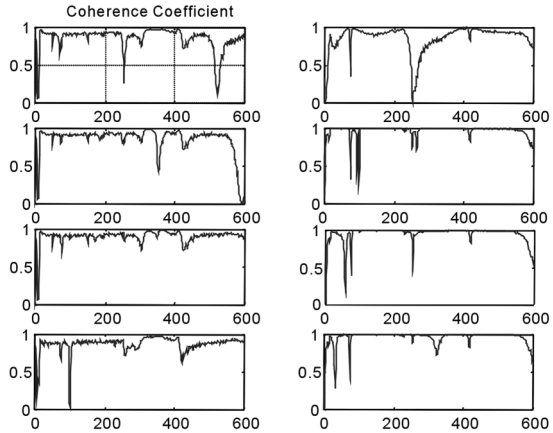

Fig. 6 (d) Input/Output coherence function (First column corresponds to the 1st excitation)

forces and four acceleration responses of the beam. The falls of coherence coefficients in Fig. 6(d) near 250 Hz and 411 Hz show that the four acceleration responses are not completely caused by the two excitations, which also accounts for the abnormal jumps of the actual identified loadings in this frequency range.

It should also be noted that the damping ratio of the steel cantilever beam is small (0.01) compared to the damping ratio (0.05) of the plastic glass beam. Because of this, the identified loadings are very sensitive to the mounting condition of the shakers, especially misalignment of the two ends of the drive rode having remarkable effects on the test results. In addition, the fixing of the shaker's drive rod to a structure is often suffered from accidental perturbations or even from elongation of the suspension rubber ropes for a period of time. To make sure that the measured responses are caused strictly by corresponding excitations, following measures have been adopted to avoid such adverse effects caused by stiffness attachment. When measuring the first column of the FRF corresponding to excitation 1 (the 1st shaker) in step 2 of section 2, the drive rod of the 2nd shaker should always keep its connection with the beam as the in-situ tests, and vice versa. In other words, the test settings while measuring the FRFs must keep the same state strictly as that when measuring the responses used for loading identification in step 3. This can be easily attained by switching on or off corresponding signal generators according to what is going to be measured, and keep the settings of other related facilities unchanged. If the FRFs and coherence functions varied during experiments, they have to be measured again after adjusting or correcting the misalignment of the drive rods.

In Fig. 6(d), the discouraging part of the coherence functions (below 10 Hz) also explains why the identification results in this frequency range are inferior to those in the other part. The quality of FRFs and coherence functions is critical to the success of loading identification. Before measuring responses and excitations in each test, FRFs and coherence functions have to be monitored for every channel by a spectrum analyzer (HP35670 in our laboratory) to make sure that they are in good status. If not, check the mounting condition of drive rods carefully, adjust them horizontally, vertically, and fasten them tightly to the structure until the values of coherence function are 1 for most of the frequency range, which indicates that the measured responses are induced by the excitations to be identified. Moreover, an adequate number of peaks should appear in the plots of the FRFs to allow the measured responses containing sufficient participating modes for loading identification.

4.3 Plastic glass cantilever beam

Similar to section 4.2, two uncorrelated excitations were applied at points 4,5 horizontally and four acceleration responses were measured at 5,7,8,11 (Fig. 3). The significant frequency range including the first four natural frequencies is from 0 to 400 Hz. The identified excitations (Fig. 7a and Fig. 7b) agree perfectly well with the actual excitations. The plastic glass cantilever beam has more damping than the steel cantilever beam and the coherence functions almost approximately equal to 1 (Fig. 7c and Fig. 7d), which explains that why the identification results (Fig. 7a and Fig. 7b) of the plastic glass cantilever beam with the same size are much better than that of the steel cantilever beam (Fig. 6a and Fig. 6b)

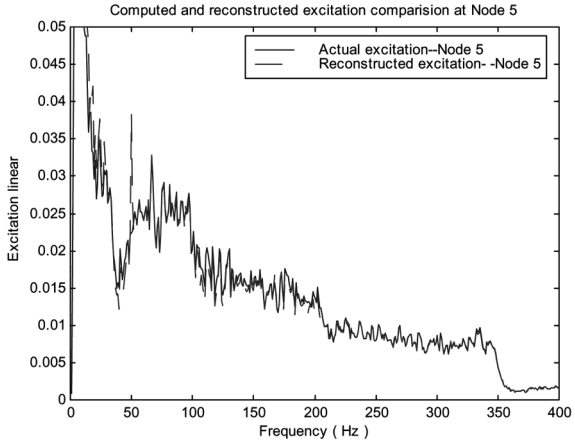

Fig. 7 (a) Point 5 identification result comparison

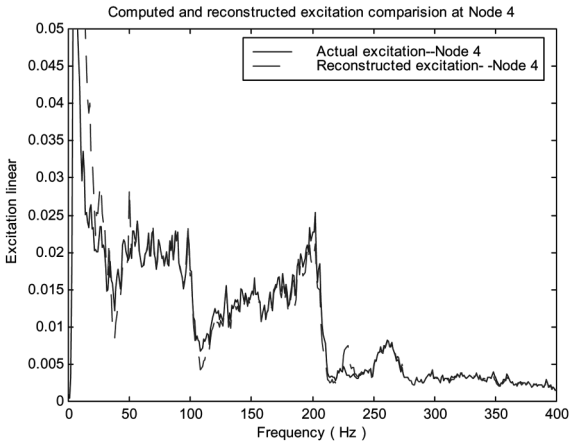

Fig. 7 (b) Point 4 identification result comparison

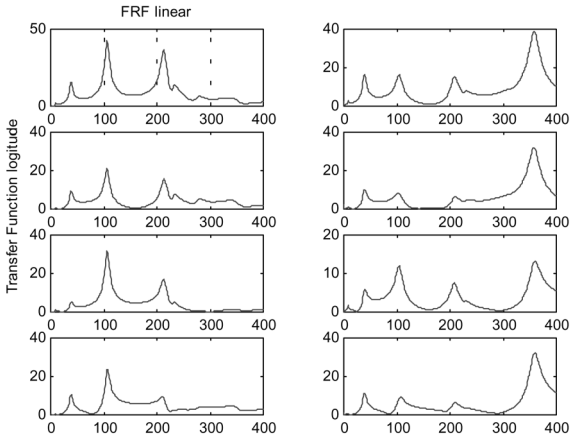

Fig. 7 (c) Frequency response function

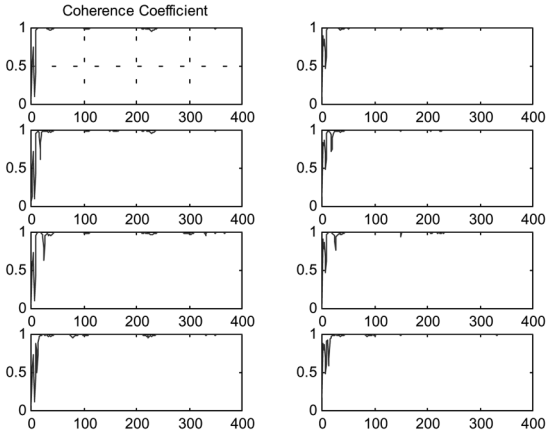

Fig. 7 (d) Input/Output coherence function

4.4 Four-story plastic glass frame

The IPEM was applied to the four-story frame, which is a complex structure made of plastic glass (Fig. 4). Its frequency range of interest is between 0 and 100 Hz, which includes the first five natural frequencies. Two excitations were applied at points 11,2 horizontally and four acceleration responses were measured at locations 7,32,40,48. The space frame was additionally excited by fully correlated excitations to compare the influences of different types of excitations on the loading identification results in addition to the uncorrelated excitations used in the above mentioned experiments.

4.4.1 Identification results for fully correlated excitations

In one case, the two excitations are fully correlated (Fig. 8a). The identified loadings are shown Fig. 8(b) and Fig. 8(c). Abnormal jumps in identification results appear more frequently, and

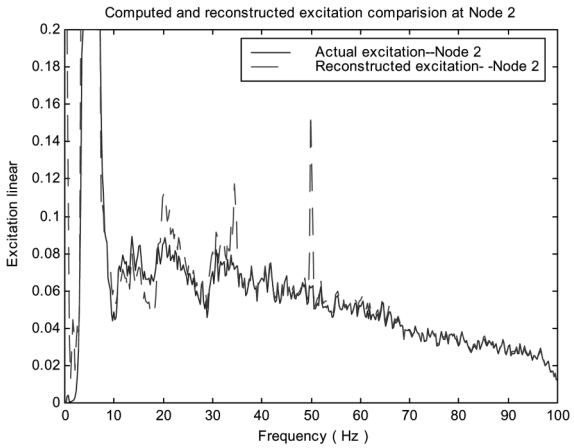

Fig. 8 (a) Point 2 reconstructed and actual force

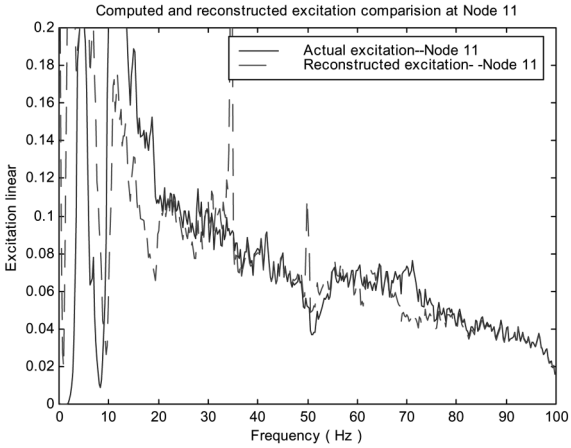

Fig. 8 (b) Point 11 reconstructed and actual force

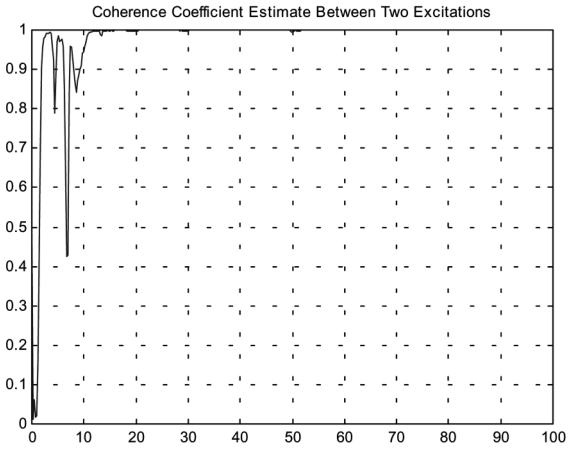

Fig. 8 (c) Measured correlation coefficients

obvious disparities of identified loadings from their actual values take place in most spectral region. The correlation function between the two excitations shows that these two forces are fully correlated in almost all the frequency range of interest as expected. In fact, the two forces were generated by the same signal generator, which were channeled to two power amplifiers with different amplitudes simultaneously.

4.4.2 Identification results for uncorrelated excitations

In the other case, the two excitations are uncorrelated (Fig. 9a). Fig. 9(b) and Fig. 9(c) show the identified loadings, which agree perfectly well with the actual ones on the whole. The correlation function between the two excitations in Fig. 9(a) reveals that the two excitations are satisfactorily uncorrelated in almost all the frequency range of interest except locally within the lower frequency part. Hence, higher identification precision is achieved for uncorrelated excitations than for fully correlated ones (Figs. 8c & d and Figs. 9c & d).

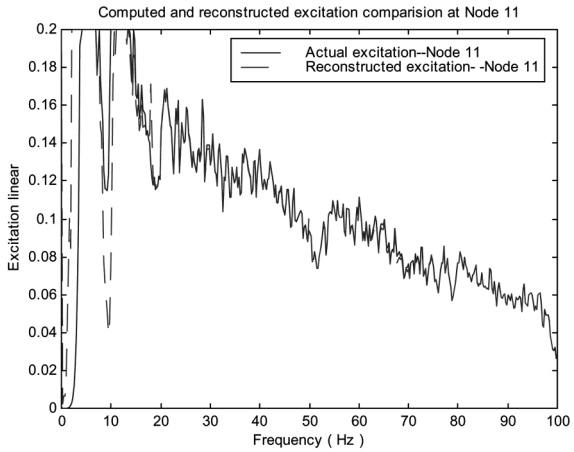

Fig. 9 (a) Point 11 reconstructed and actual force

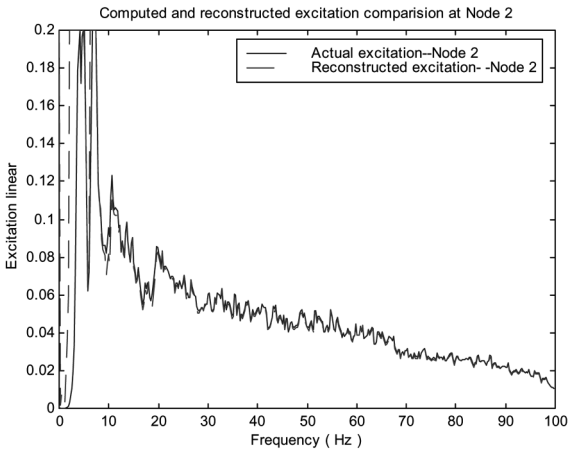

Fig. 9 (b) Point 2 reconstructed and actual force

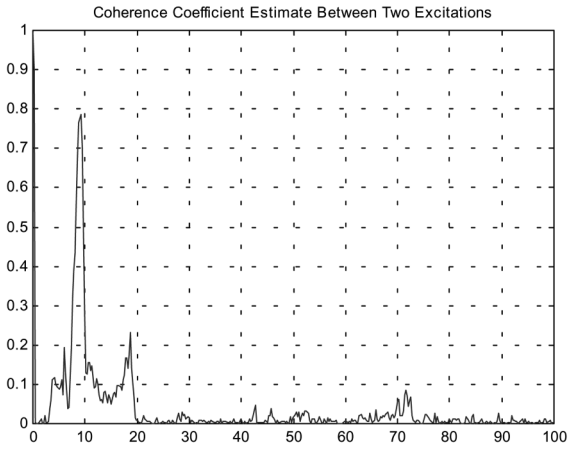

Fig. 9 (c) Measured correlation coefficients of two uncorrelated excitations

5. Influences of the number of response measurement points and noise contamination on the precision of identification results

The precision of loading identification is influenced both by the number of response measurement points and measurement noise. In above experiments, four acceleration responses were measured to identify the loadings and the redundancy degree, i.e., the number of responses more than the number of excitations, is two. Actually, six responses had been totally measured during the tests on the plastic glass space frame in the cased of uncorrelated excitations. The other two measured responses were at point 11,2, which were called drive points where the drive rod excites the frame laterally. Thus, it is possible to compare the effects of redundancy degrees on the precision with which the excitation PSD matrix is identified.

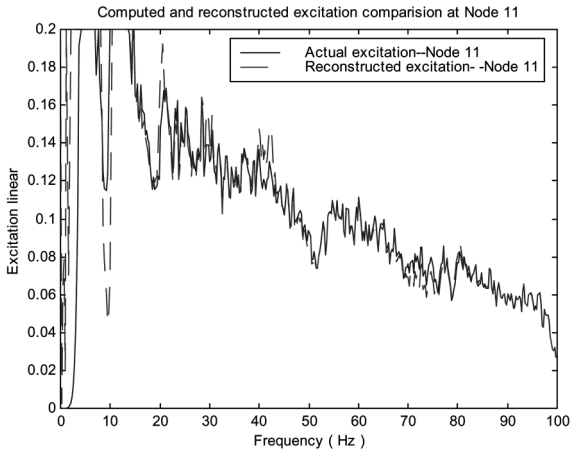

Fig. 10 (a) Identification results at point 11 with only two measurement points 2,11

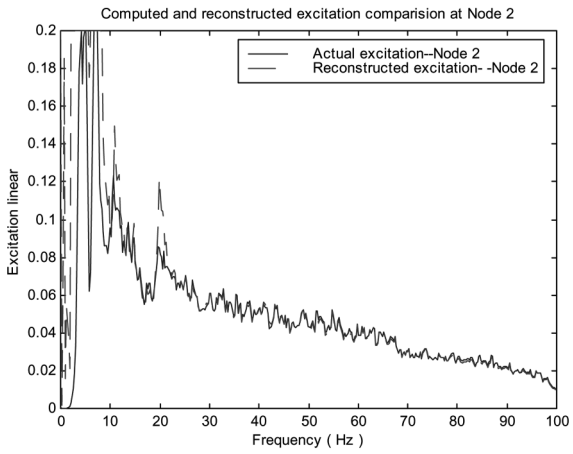

Fig. 10 (b) Identification results at point 2 with only two measurement points 2,11

5.1 The influence of the number of response measurement points on the identification precision

In Fig. 10(a) and Fig. 10(b), only two measured responses at points 11,2 were used in the identification. Under this circumstance, the number of response measurements (two) equals to the number of excitations (two), no redundancy exists. The identification results are not so good as the results obtained from four responses because of the abnormal jumps and disparities. This validates a common inference that adequate redundancy of response measurement points yields better experiment results.

However, more redundancy degree does not always guarantee better identification results. When five or six response measurements are taken into consideration, the identified loadings are similar to those by four responses (Fig. 9b and Fig. 9c) without much improvement. In addition, computations demonstrate that drive points, as 11 or 2 in this example, may probably have better identification results than the other points.

5.2 The effect of noise in measurement on the identification precision

The precision of loading identification is not only affected by the degree of response measurement redundancy, but also by the measurement noise. First, consider the effect of noise contamination of the actual measured response signals when only the responses contain 30% random white noise with respect to its maximum amplitude and there is no noise contamination in the FRFs and excitation data. The identification results are shown in Fig. 11(a) and Fig. 11(b). The noise at the lower frequencies will cause significant errors, whereas the noise at other frequency range does not.

Next, consider that only the FRFs are contaminated by the measurement noise. The identified loadings shown in Fig. 11(c) and Fig. 11(d) are based on the FRFs with 30% random white noise and there is no random noise in the measured excitations or responses. In this case, the identification errors are distributed evenly over the entire frequency range, unlike the above case in which only the responses are polluted with noise. When measurement noise is involved in both the

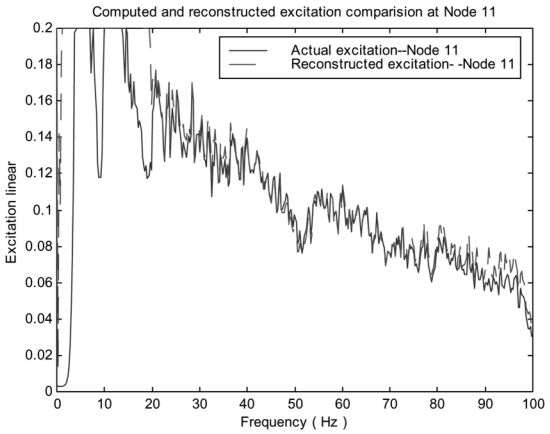

Fig. 11 (a) Identified result at point 11

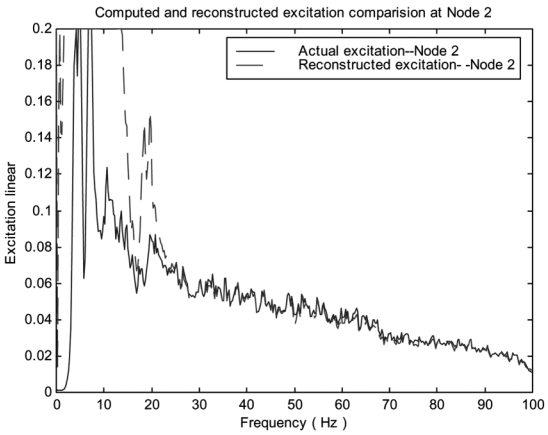

Fig. 11 (b) Identified result at point 2

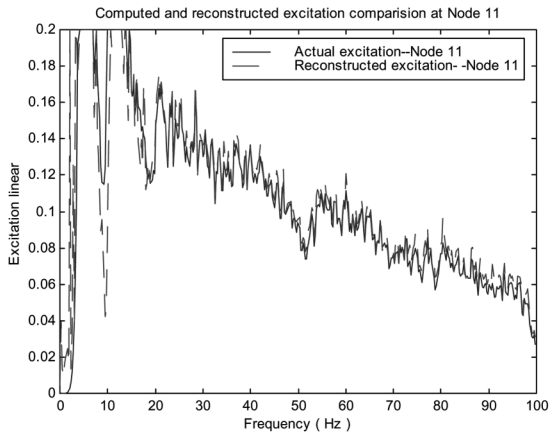

Fig. 11 (c) Identified result at point 11

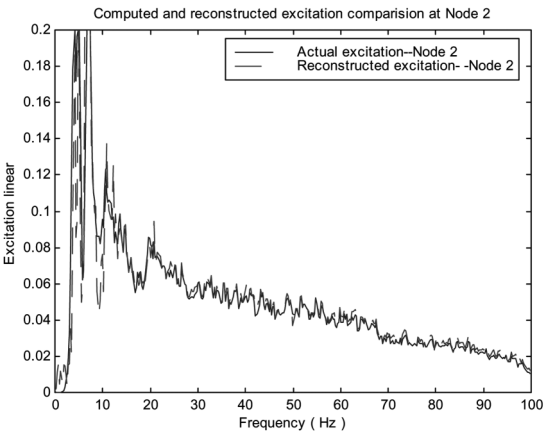

Fig. 11 (d) Identified result at point 2

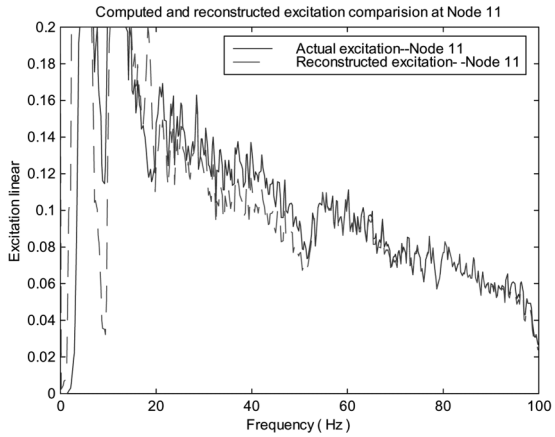

Fig. 11 (e) Identified result at point 11 with 10% calibration error at Ch.6

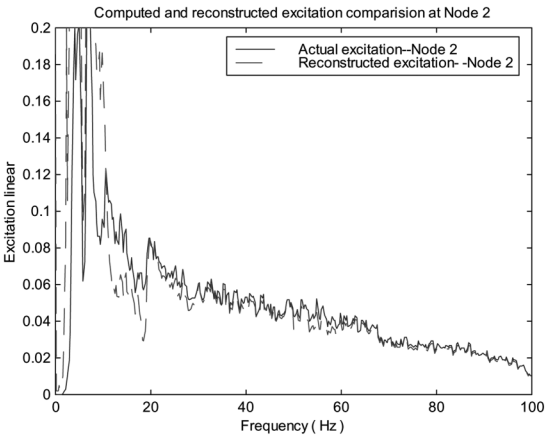

Fig. 11 (f) Identified result at point 2 with 10% calibration error at Ch.6

responses and the FRFs, the identification results are similar to the case of only responses with random noise.

After a detailed analysis, it was found that the contaminated response auto PSD matrices only had a variation of no more than 0.5 percent even when subjected to contamination by 30 percent random white noise. When calculating the FRF matrices, excitation and response auto PSD matrices from the time histories, they were all averaged for fifty times. Because of this, the random noise contamination was almost smoothed out by averaging. This is why the IPEM is robust to random noise.

Finally, consider the accelerometers having ten percent null drift or zero-drift errors, which often happens during instruments calibration, i.e., all measured acceleration responses will be a hundred and ten percent of their actual values. Fig. 11(e) and Fig. 11(f) show the identification results in which the disparities increase even if one accelerometer is subjected to such calibration error.

6. Conclusions

The inverse pseudo excitation method was implemented for loading identification experiments on three structures subjected to stationary random excitations. The identified loadings agree quite well with actual uncorrelated excitations. This method is not only computationally efficient and accurate to identify unknown random excitations, but robust to random noise.

Although immune to random noise, the IPEM is severely affected by system calibration errors. A certain degree of redundancy is beneficial to the precision of loading identification. Moreover, the accuracy of FRF measurement is critical to the success of loading identification, and more structural damping leads to better identification results.

However, the singularity of the FRF matrices near some resonant frequencies is not completely solved even though SVD is introduced. Epsilon decomposition method is an appealing way to solve this problem if epsilon could be effectively determined. Other existing problems are that sometimes the force positions are not known, and that the calibration FRFs (Step 2 of section 2) cannot be measured in-situ accurately if the mounting places are not accessible or the working conditions offend in some situations.

Acknowledgements

The authors acknowledge for the joint support of the Natural Science Foundation of LiaoNing (No. 20032120), support of the Construction Administration of LiaoNing (No. 02001), and Young Teacher's Foundation of Dalian University of Technology. The authors are also grateful for the support of Professor Peter Avitabile from University of Massachusetts Lowell, who sent to us one of his latest articles and related lecture notes for our reference, and the generous help from Professor Jia-Hao Lin in our department for the improvement of the manuscript, and Professor Wan-Xie Zhong for his inspiring instructions.

References

Adams, Robert and Doyle, James F. (2002), "Multiple force identification for complex structures", *Experimental*

Mechanics, **42**(1), 25-36.
Avitabile, P. and Chandler, D. (2001), "Selection of measurement references using the TRIP method", *Proc. of 19th Int. Modal Analysis Conf.*, Florida, U.S.A.
Barlett, F.D. and Flannelly, W.G. (1979), "Modal verification of force determination for measuring vibratory loads", *J. of the American Helicopter Society*, **19**(4), 10-18.
Bendat, J.S. and Piersol, A.G. (2000), *Random Data: Analysis and Measurement Procedures*, John Wiley & Sons, Inc., New York.
Callahan, O.J. and Piergentili, F. (1994), "Force estimation using operational data", *Proc. of 8th Int. Modal Analysis Conf.*, 1586-1592.
Desanghere, G. and Snoeys, R. (1985), "Indirect identification of excitation forces by modal coordinate transformation", *Proc. of 3rd Int. Modal Analysis Conf.*, 685-690, Florida, U.S.A.
Dobson, B.J. and Rider, E. (1990), "A review of the indirect calculation of excitation forces from measured structural response data", *J. Mech. Eng. Sci. : Part C*, **204**, 69-75.
Ewins, D.J. (1984), *Modal Testing: Theory and Practice*, Research Studies Press Ltd., London.
Giansante, N., Jones, R. and Galapodas, N.J. (1982), "Determination of in-flight helicopter loads", *J. of the American Helicopter Society*, **27**(3), 58-64.
Golub, G.H. and Van Load, C.F. (1996), *Matrix Computation*, The Johns Hopkins University Press.
Hillary, B. and Ewins, D.J. (1984), "The use of strain gages in force determination and frequency response measurements", *Proc. of 2nd Int. Modal Analysis Conf.*, 627-634, Florida, U.S.A.
Juang, J.N. (1994), *Applied System Identification*, PTR Prentice-Hall, Inc., New Jersey.
Karl, S.K. (1987), "Force identification problems-An overview", *Proc. of the 1987 Society of Experimental Mechanics Spring Conf. on Experimental Mechanics*, 838-844, Florida, U.S.A.
Li, D.S. and Guo, X.L. (2003), "Loading identification of random excitations", *Proc. of 21th Int. Modal Analysis Conf.*, Florida, U.S.A.
Lin, J.H. (1992), "A fast CQC algorithm of PSD matrices for random seismic responses", *Comput. Struct.*, **44**, 683-687.
Lin, J.H., Zhang, W.S. and Li, J.J. (1994), "Structural responses to arbitrarily coherent stationary random excitations", *Comput. Struct.*, **50**(5), 629-633.
Lin, J.H., Guo, X.L., Zhi, H., Howson, W.P. and Williams, F.W. (2001), "Computer simulation of structural random loading identification", *Comput. Struct.*, **79**, 375-387.
Newland, N.E. (1984), *An Introduction to Random Vibration and Spectral Analysis*, Longman, London.
Okubo, N., Tanabe, S. and Tatsuno, T. (1985), "Identification of forces generated by a machine under operation condition", *Proc. of 3rd Int. Modal Analysis Conf.*, 920-927, Florida, U.S.A.
Zhu, X.Q. and Law, S.S. (2002), "Moving loads identification through regularization", *J. Eng. Mech.*, **128**(9), 989-1001.